Case Report

Multiple skull fractures of a horse after a traumatic event

Patient identification, history and clinical findings

A 15-year-old Belgian Warmblood gelding used for combined driving was presented with a head trauma after receiving a kick from another horse.

On the clinical examination the horse presented bilateral epistaxis, absence of airflow on the right nasal passage (NP), diminished airflow on the left NP with abnormal respiratory noise and dyspnoea. There was a bone depression on the axial and right aspects of the nasal bone (NB) midway between the nostrils and the facial crest. There was no swellings or wounds present. The remainder of the clinical exam and the neurological examination were unremarkable.

A nasopharynx tube was placed on the left NP to ensure normal airflow.

Ancillary diagnostic tests

1.Radiographic study – Figures 1. to 6.

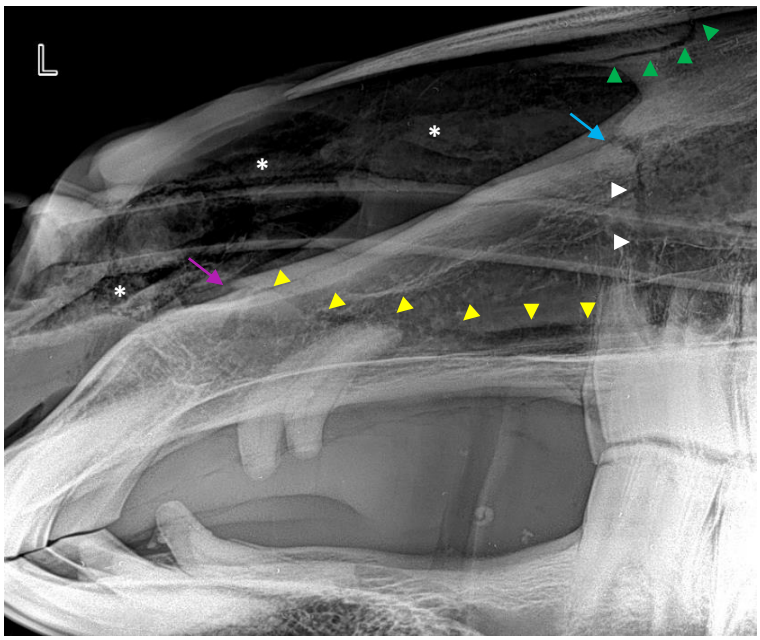

Figure 1. Latero-lateral radiographic view of the rostral aspect of the horse's skull. The cassette was positioned on the left side (L) of the head. Rostral is to the left and dorsal is to the top. Detailed image description is presented later on.

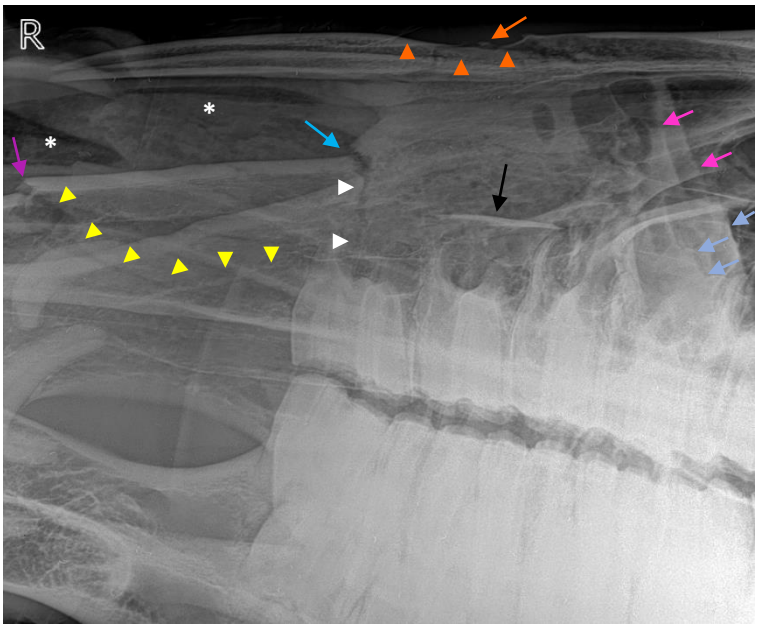

Figure 2. Left latero30ºdorsal-right lateroventral oblique radiographic view of the horse's skull. Rostral is to the left and dorsal is to the top. Detailed image description is presented later on.

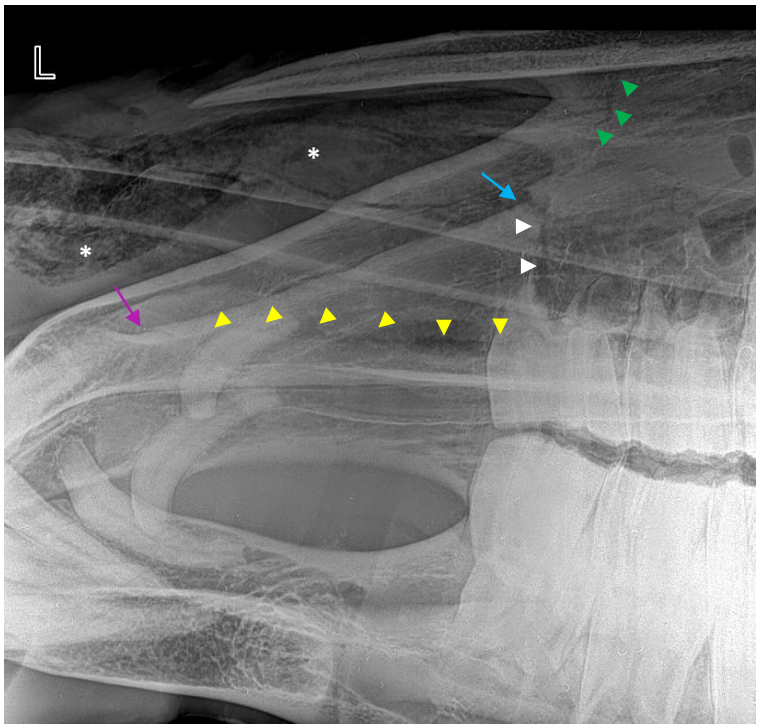

Figure 3. Right latero30ºdorsal-left lateroventral oblique radiographic view of the rostral aspect of the horse's skull. Rostral is to the left and dorsal is to the top. Detailed image description is presented later on.

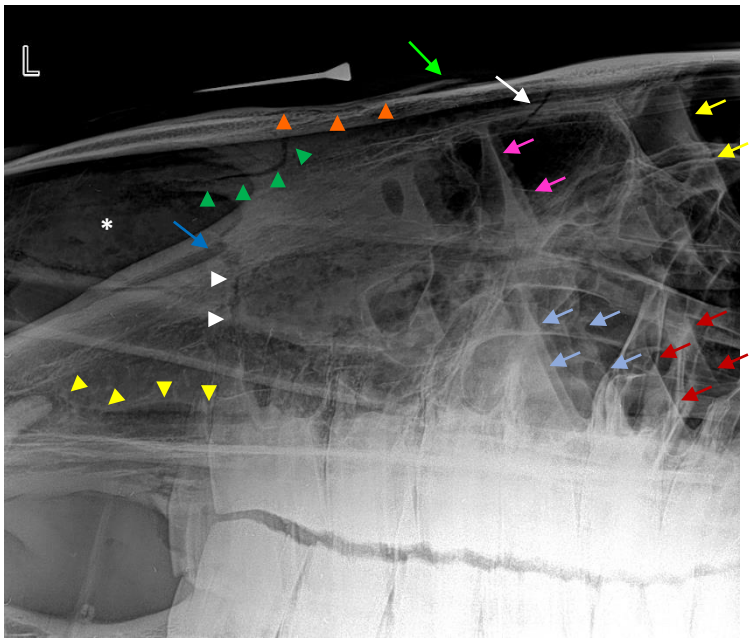

Figure 4. Latero-lateral radiographic view of the horse's skull. The cassette was positioned on the left side (L) of the head. Rostral is to the left and dorsal is to the top. Detailed image description is presented later on.

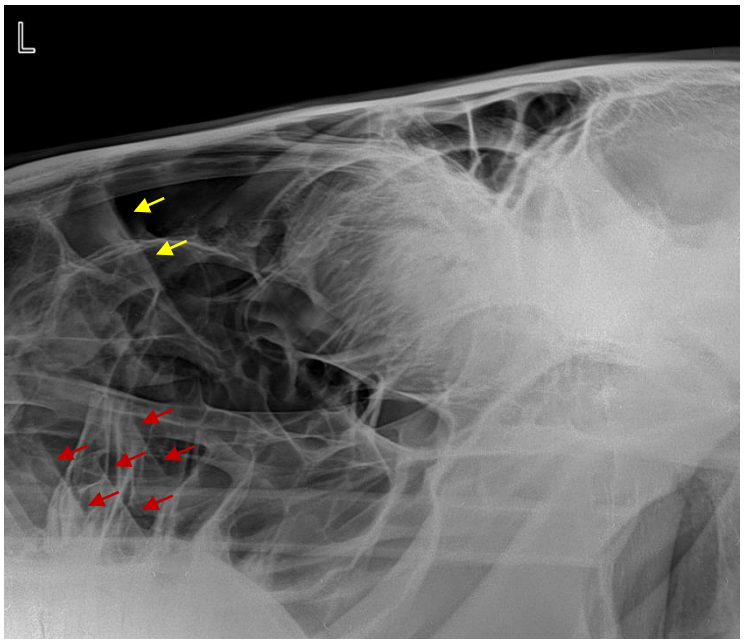

Figure 5. Latero-lateral radiographic view of the horse's skull. The cassette was positioned on the left side (L) of the head. Rostral is to the left and dorsal is to the top. Detailed image description is presented later on.

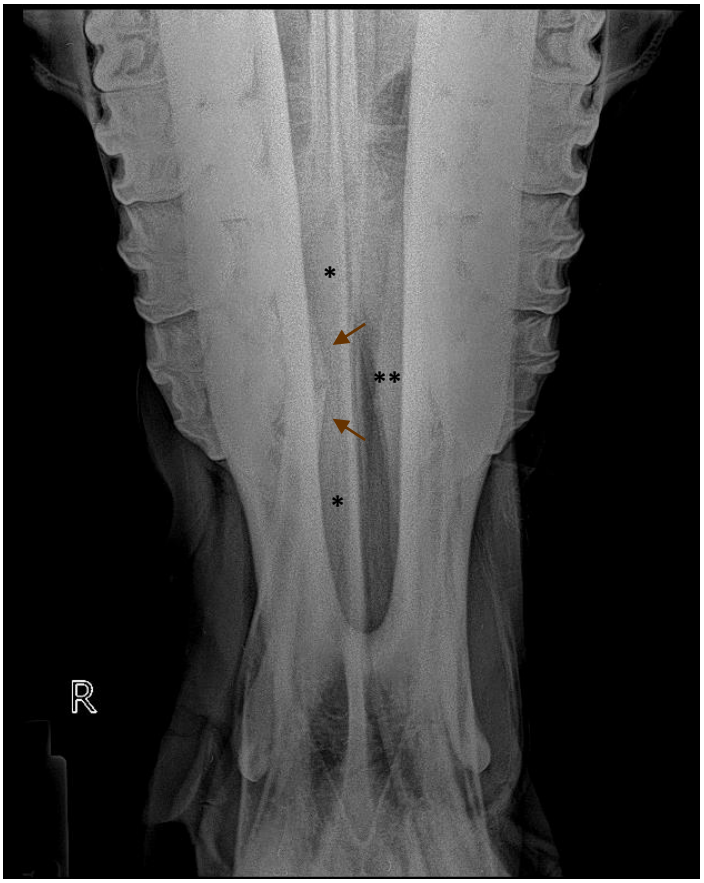

Figure 6. Dorsoventral radiographic view of the rostral aspect of the horse's skull. Right (R) is to the left and caudal is to the top. Detailed image description is presented later on.

Radiation safety

All personnel used lead aprons, thyroid guards and dosemeters; the cassette holder also used lead gloves.

Patient preparation

The horse was placed in stocks and sedated intravenously with romifidine 0.02mg/Kg (Sedivet®BoehringerIngelheim) and butorphanol 0.01mg/K (Butomidor®richterfarma); a rope head collar and a head stand were used.

Equipment

Direct digital radiography system.

Case Report

Multiple skull fractures of a horse after a traumatic event

Image critique

View	Collimation	Positioning	Centering	Exposure	Artifacts
Latero-lateral (Figure 1.)	Adequate	Slight rostral-to-caudal and dorsal-to-ventral obliquity	Adequate	Adequate (65 kV; 8.0 mAs)	Two ill-defined radiopacities rostrad to 306/406 [modified Triadan system (Appendix, Figure 1.) used henceforth] and other rostrad to 304/404; *
Left latero30ºdorsal-right lateroventral oblique (Figure 2.)		Adequate	Should be centered slightly rostrad		*
Right latero30ºdorsal-left lateroventral oblique (Figure 3.)			Adequate		
Latero-lateral (Figure 4.)		Moderate right dorsal-to-left ventral and rostral-to-caudal obliquity			Ill-defined rounded radiopacity rostrad to 306/406; Radiopaque marker (metallic mail) at the level of the NB depression; *
Latero-lateral (Figure 5.)		Moderate dorsal-to-ventral obliquity			*
Dorsoventral (Figure 6.)		Adequate		Adequate (75 kV; 8.0 mAs)	

* Nasopharynx tube (two wide parallel radiopaque lines with a radiolucent space between) placed on the left ventral meatus, from the left nostril till the nasopharynx.

Table 1. Image critique of the radiographic exam (Figures 1. to 6.). that includes the description of the views, appreciation of the collimation, positioning, centering and exposure and description of the artifacts present.

Case Report

Multiple skull fractures of a horse after a traumatic event

Image description

Figure 1.

1.a. Well-defined wide radiolucent line (RL) with a horizontally inverted L-shape on the NB, dorsal and caudal to the nasoincisive notch (NIN) (green arrowheads);

1.b. Diffuse heterogeneous increased soft-tissue opacity (STO) on the nasal passages (NPs) (asterisks);

1.c. Dorsorostral-to-ventrocaudal oblique irregular thin RL on the nasal process of the incisive bone (NPIB) between 103/203 and 104/204 (purple arrow), that continues obliquely, caudally and ventrally as an irregular RL on the maxillary bone (MB), dorsally to 104/204; starts to be wider and horizontal midway between 104/204 and 106/206 and continues until the level of the roots of 106/206 (yellow arrowheads); continues as a vertical, wide, irregular RL (white arrowheads) until the dorsal border of the incisive bone (IB), where there is a dorsorostral-to-ventrocaudal oblique irregular bone discontinuity (blue arrow).

Figure 2.

2.a. Concave depression on the right NB at the level of 107/207 (orange arrowheads) with a small ill-defined radiopacity at its base (orange arrow);

2.b. Same as 1.b.;

2.c. Same as 1.c.; this view confirms that the radiolucent lines (RLs) are ubicated in the right NPIB and right MB;

2.d. Well-delimitated spiculated thin longitudinal bony radiopacity dorsally to the roots of 107 (black arrow);

2.e. Multiple fluid lines (FL), with increased STO below them, in the dorsal nasal conchal bullae (DNCB) (pink arrows) and rostral maxillary sinuses (RMS) (blue arrows).

Figure 3.

3.a. Thin well-delimitated vertical RL on the NB, caudally to the left NIN, with two thin horizontal RLs rostrally (green arrowheads);

3.b. Same as 1.b. and 1.c/2.c..

Figure 4.

4.a. Same as 1.a. and 1.b.;

4.b. Same as 2.a. (metallic marker); however, the radiopacity at its base is not seen and there is another well-defined wide horizontal RL on the NB, caudally to the depression (green arrow);
4.c. Curved RL line with a dorsocaudal-to-rostroventral obliquity ventrally that finishes as a vertical line on the NB dorsally to the DNCB (white arrowhead);
4.d. Same as 1.c. (only caudally to 104/204);
4.e. Same as 2.e.; there are also multiple FL in the conchofrontal sinuses (CFS) (yellow arrows) and caudal maxillary sinuses (CMS) (red arrows).

Figure 5.
5.a. Multiple FL in the CFS (yellow arrows) and CMS (red arrows).

Figure 6.
6.a. Two triangular-shaped bone radiopacities on the axial aspect of the right maxilla at the level of 106 (browns arrows);
6.b. Diffuse (solitary asterisks) and localized (double asterisks) increased STO on the right and left NP, respectively.

Diagnosis/differential diagnoses

- The RLs evident on the right IB and MB are compatible with a large fragment (detailed in 1.c./2.c./4.d.) displaced dorsally in its rostral aspect and ventrally in its caudal aspect;
- The RLs on the NB (detailed in. 1.a./2.a./3.a.) are compatible with bone fissures/fractures in that locations;
- The presence of epistaxis can indicate that the fractures penetrated the mucosal lining of the NPs and/or the paranasal sinuses (PS) (Levine 1997; Barber 2005), with consequent collection of blood/sanguinolent material, causing the diffuse increased STO on the NPs (Figures 1. To 4. and 5.) and the FL in the PS (Figures 2. to 5.), respectively [Differential diagnosis for FL in the PS: thickening of the sinus mucosa, purulent material, masses (Barakzai 2014)];
- The dyspnoea and the absence/diminishment of airflow through the NPs may be a consequence of the presence of blood clots, narrowing of the NPs secondary to the displaced fractures (Dowling *et al.* 2001; Burba and Collier 1991) or inflammation/oedema of the mucosa.

Treatment

Flunixin-meglumine (Nixyvet®DFV 1,1 mg/Kg) and dexamethasone (Caliercortin®Calier 0.1 mg/Kg) were administered intravenously at arrival. Phenylbutazone (EqZone®Calier) was administered orally, twice daily, during 10 days: 3 days at 4,4mg/Kg and 7 days at 2.2mg/Kg.
The airflow on both NPs improved progressively, so the nasopharynx tube was removed 4 days after arrival. An upper respiratory tract endoscopy was performed and the most clinically significant finding was narrowing of the right NP.

Despite of the initial clinical improvement, the horse was referred to perform a computed tomography (CT) under sedation because radiography almost always underestimates the degree of damage in these cases (Barazkai 2014), and it was imperative to determine the involvement of other structures, fractures/fragments displacement and affection of the NPs.

2.Computed Tomography

The most significant findings were the following (detailed description in Appendix - Figures 2. to 7.):

- Large moderately medially displaced bone fragment on the right rostral IB and MB (Figure 7.);
- Multiple medially displaced fragments on the right caudal MB and NB, partially invading the interior of the right ventral nasal concha (VNC) (Figure 8.);
- Fracture of both nasal bones (Figure 9.);
- Fissure on the left IB (Figure 10.)
- Presence of material in the ventral conchal sinuses (VCS) and RMS (Figure 11.) and dorsal and ventral nasal conchal bullae on both sides (Figure 12.).

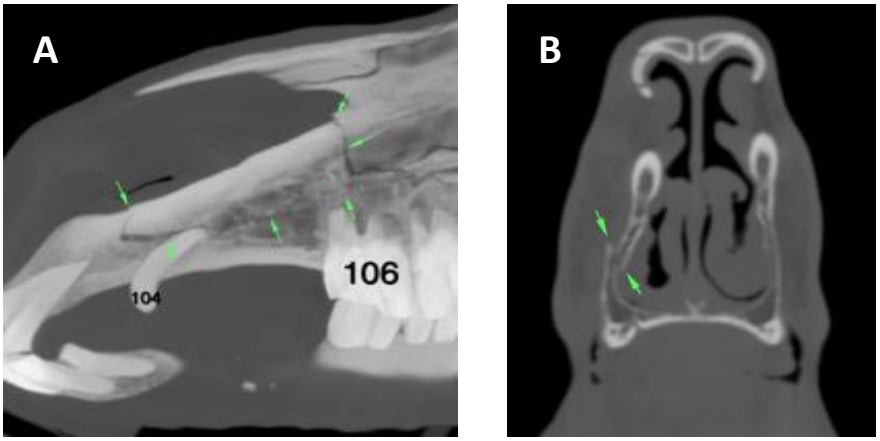

Figure 7. Maximum intensity projection reconstruction (A.) and transverse CT section image (B.) of the rostral aspect of the head. There is a thin, irregular hypoattenuating line at the nasal process of the right incisive bone, that starts at the level 103-104 interdental space and extends caudally, dorsally to the root of the 104, and continues further caudally with a horizontally path through the maxillary bone (A.), with moderate medial displacement of the main fragment (B.). At the level of 106 an additional vertical hypoattenuating line crosses the nasal process of the incisive bone finishing at its dorsal border, rostrally to the nasoincisive notch, and delimitating a fragment of big dimensions (9 x 3 cm) (A.). Rostral is to the left on image A. and right is to the left on image B.

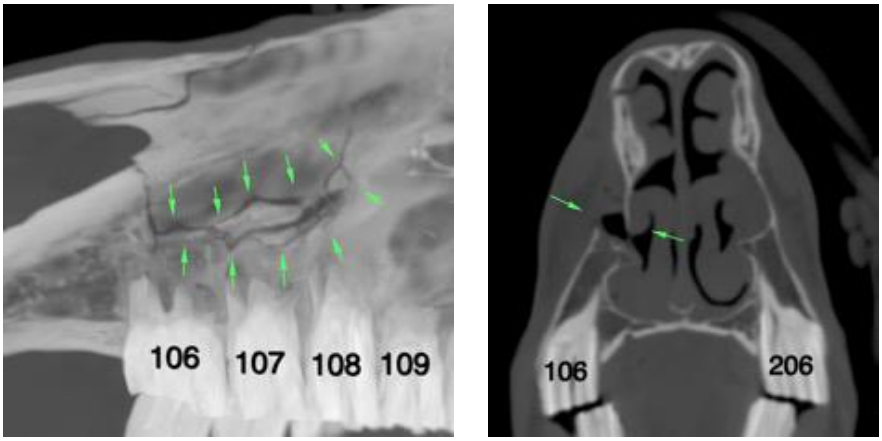

Figure 8. Maximum intensity projection reconstruction (A.) and transverse CT image CT (B.) images of the horse's head. From the level of 106, the horizontal fracture line continues caudally, much wider than rostrally, and contains multiple small fragments (A. and B.). These fragments are medially displaced, involving the right ventral nasal concha and its bulla. This fracture is dorsal to the maxillary check teeth roots along its trajectory. At the level of 108 itinvolves the infraorbital canal, which is partially narrowed. From this point caudally, the fracture continues dorsally in the direction of the nasal bone, where it ends (A.). Rostral is to the left on image A. and right is to the left on image B..

Figure 9. Three-dimensional reconstruction of the horse's head. The fracture of the right nasal bone originates at the ventrolateral border of the bone, dorsally to the nasoincisive notch, and continues caudally. The dorsal line is thinner and converge with the ventral line approximately at the level of 107. From this point the fracture continues further caudomedially with a curve path. At midline it crosses to the left nasal bone, where it continues caudolaterally until the level of 208, where it turns ventrally, and finishes at the level of the nasomaxillary suture. Right is to the left.

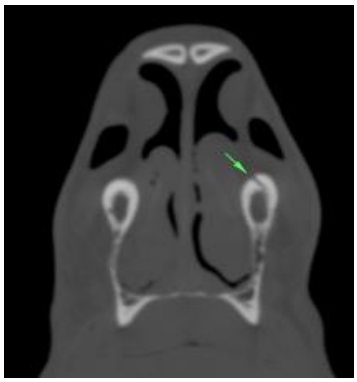

Figure 10. Transverse section CT image of the head at the level of the 204-206 interdental space showing a fissure line that originates at the lateral cortex of the dorsal border of the nasal process of the left incisive bone. Right is to the left.

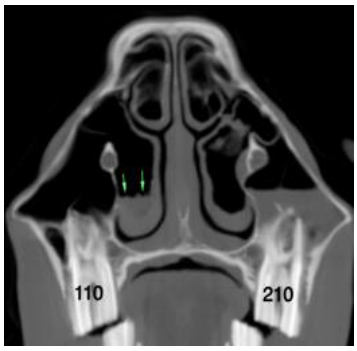

Figure 11. Transverse section CT image of the horse's head at the level of 110/210. There is a small amount of soft-tissue attenuating material at the dependent aspect of the ventral conchal and rostral maxillary sinuses, with a flat dorsal border (fluid line). Right is to the left.

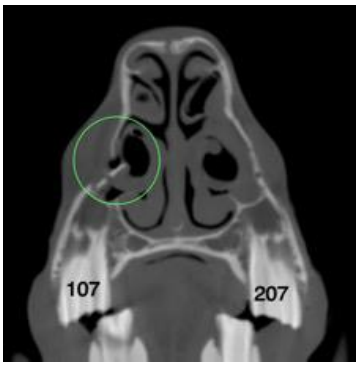

Figure 12. Transverse section CT image of the horse's head at the level of 107/207. There is moderate amount of soft-tissue attenuating material within the dorsal and ventral nasal bullae. The ventral nasal conchal bulla contains several bone fragments from the maxillary bone fracture (green circle). Right is to the left.

The case was managed conservatively due to the favourable clinical improvement, horse's age and owner's decision. However, reconstruction of the nasal bridge could have been important to enable normal airflow, the blood clots/debris could have been lavaged from the sinuses and NPs (Tremaine 2004) and systemic antibiotics could have been indicated (Barber 2005).

The horse started to work 6 weeks after the traumatic event, despite of the recommendation to perform a clinical and radiographic control before resume exercise. According to the owner the horse is fully recovered and working at the previous level.

Critical reflection

The author considers the imaging approach adequate because the radiographic study was complete and well-executed, although an additional dorsoventral projection at the level of the PS could have been useful to evaluate the VCS, and a CT was also performed.

The decision to perform the CT was of great importance because allowed the identification of pathology not appreciated/completely diagnosed in the radiographic exam, the most important being the medial displacement of the bone fragment of the right rostral IB and MB and the presence of multiple medially displaced fragments on the right caudal MB and NB, partially invading the interior of the right VNC, which justifies the narrowing of the right NP.

Regarding the last finding, the radiographic exam allowed the identification of two MB fragments invading the right NP (Figure 6.) and a linear fragment dorsal to 107 (Figure 2.), that possibly represent part of the fragments identified in the CT. Furthermore, reviewing the radiographic images, there is a wide horizontal RL on the MB, dorsally to 106 and 107 (Figures 1., 3. and 4.), that went unnoticed initially, that is compatible with the rostral aspect of the fracture line diagnosed in the CT, but the author was not able to identify the other fractures/fragments.

Skull fractures are difficult to assess radiographically because of the complex morphology of the bones and superimposition of numerus structures (Bar-Am *et al.* 2008). In a recent study about the role of head CT in equine practice, CT allowed to identify a greater number of fragments and showed bone fractures not visible radiographically (Manso-Díaz *et al*. 2015), as occurred in this case.

In conclusion, CT gives more information regarding fracture configuration, structures involved and severity when compared with radiography. Therefore, CT should be the modality of choice for determining the treatment plan and the prognosis (Crijns *et al.* 2017) and in the author's opinion it is highly recommended in this type of complex cases.

Word count: 1516

References

Bar-Am, Y., Pollard, R. E., Kass, P. H. and Verstraete, F. J. M. (2008) “The diagnostic yield of conventional radiographs and computed tomography in dogs and cats with maxillofacial trauma”, *Veterinary Surgery,* 37, pp. 294-299

Barazkai, S. (2014) “Radiology of equine cheek teeth and sinus disorders”, *In Practice,* 36, pp. 46-474

Barber, S. M. (2005) “Management of neck and head injuries”, *Veterinary Clinics - Equine Practice*, 21, pp. 191-215

Burba, D. J. and Collier, M. A. (1991) “T-plate repair of fractures of the nasal bones in horses”, *Journal of the American Veterinary Medicine Association,* 7, pp. 909-912

Crijns, C. P., Weller, R., Vlaminck, L., Verschooten, F., Schauvliege, S., Powell, S. E., van Bree, H. J. J. and Gielen, I. M. V. L. (2017) “Comparison between radiography and computed tomography for diagnosis of equine skull fractures”, *Equine Veterinary Education,* doi: 10.1111/eve.12863

Dixon, P. M. and Gerard, M. P. (2019) ‘Oral cavity and salivary glands’, in Auer, J. A., Stick, J. A., Kümmerle, J. M. and Prange, T. (eds.) *Equine Surgery,* fifth edition. St. Louis, Missouri: Elsevier Saunders, pp. 441-462

Dowling, B. A., Dart, A. J. and Trope, G. (2001) “Surgical repair of skull fractures in four horses using cuttable bone plates”, *Australian Veterinary Journal,* 79, pp. 324-327

Levine, S. B. (1997) “Depression fractures of the nasal and frontal bones of the horse”, *Journal of Equine Medicine and Surgery,* 3, pp. 186-190

Manso-Díaz, G., García-López, J. M., Maranda, L. and Taeymans, O. (2015) “The role of head computed tomography in equine practice”, *Equine Veterinary Education,* 27(3), pp. 136-145

Tremaine, H. (2004) “Management of skull fractures in the horse”, *Clinical Practice - Equine Practice,* 26(4), pp. 214-222

Appendix

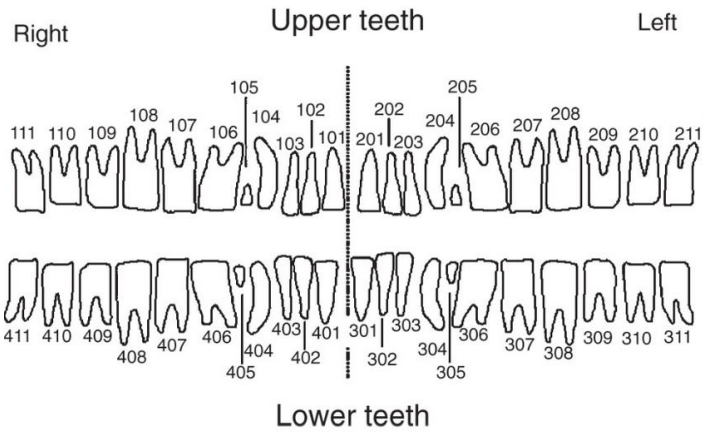

Figure 1. Modified Triadan system of equine dental nomenclature.

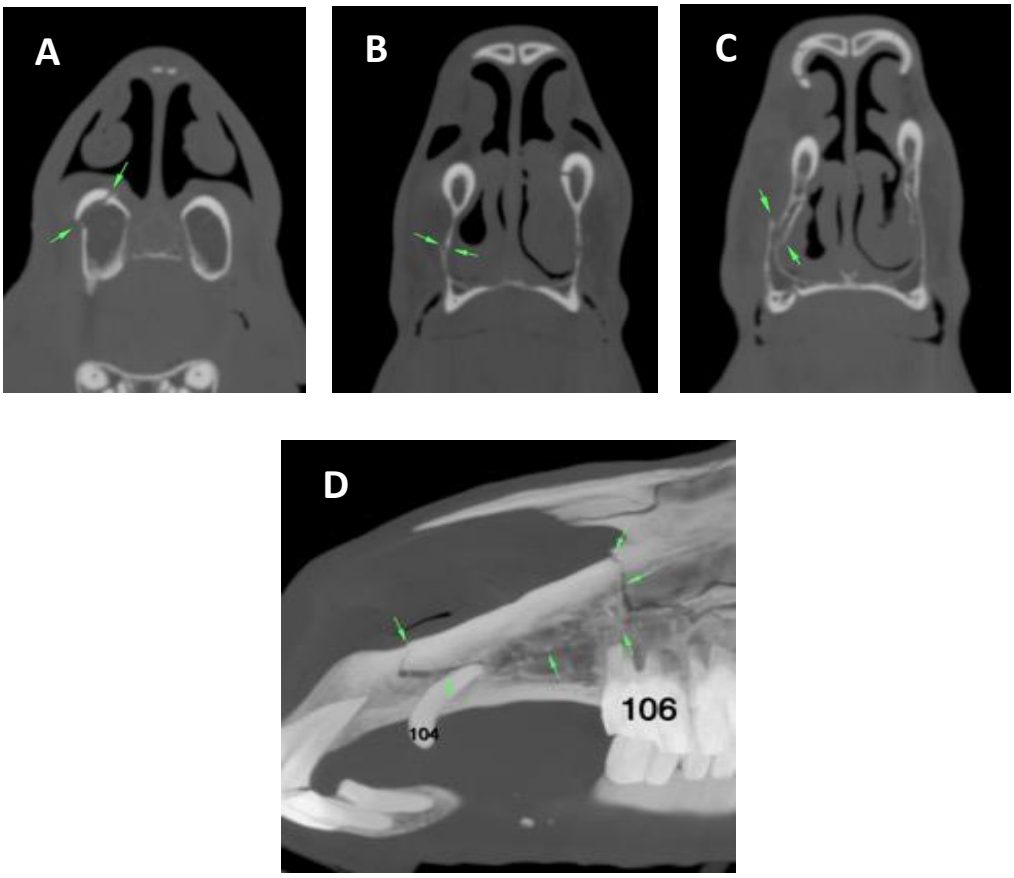

Figure 2. Transverse CT images (A., B. and C.) and maximum intensity projection reconstruction (D.) of the rostral aspect of the head. There is a thin, irregular hypoattenuating line at the nasal process of the right incisive bone, that starts at the level of the 103-104 interdental space (A. and D.) and extends caudally, dorsally to the root of the 104, and continues further caudally with a horizontally path through the maxillary bone, with moderate medial displacement of the main fragment (B., C. and D.). At the level of 106 and additional vertical hypoattenuating line crosses the nasal process of the incisive bone finishing at its dorsal border, rostrally to the nasoincisive notch, and delimitating a fragment of big dimensions (9 x 3 cm) (D.). Right is to the left on images A. to C. and rostral is to the left on image D.

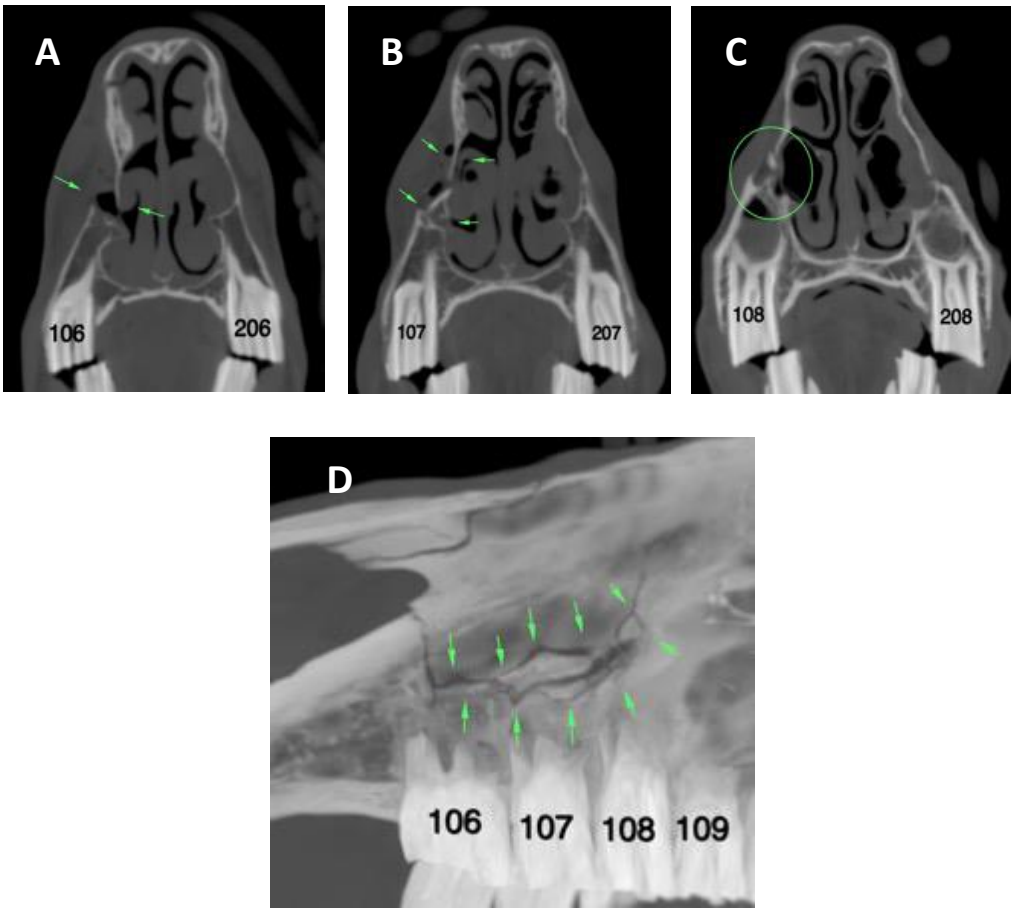

Figure 3. Transverse CT images (A., B. and C.) and maximum intensity projection reconstruction (D.) of the head. From the level of 106, the horizontal fracture line continues further caudally (A. and D.), which wider than rostrally and contains multiple small osseous fragments (B. and D.). These fragments are medially displaced, involving the right ventral nasal concha and its bulla (B.). This fracture is dorsal to the maxillary cheek teeth roots along its trajectory. At the level of 108 it involves the infraorbital canal, which is partially narrowed (C.). From this point caudally, the fracture continues dorsally in the direction of the nasal bone, where it ends. Right is to the left on images A. to C. and rostral is to the left on image D.

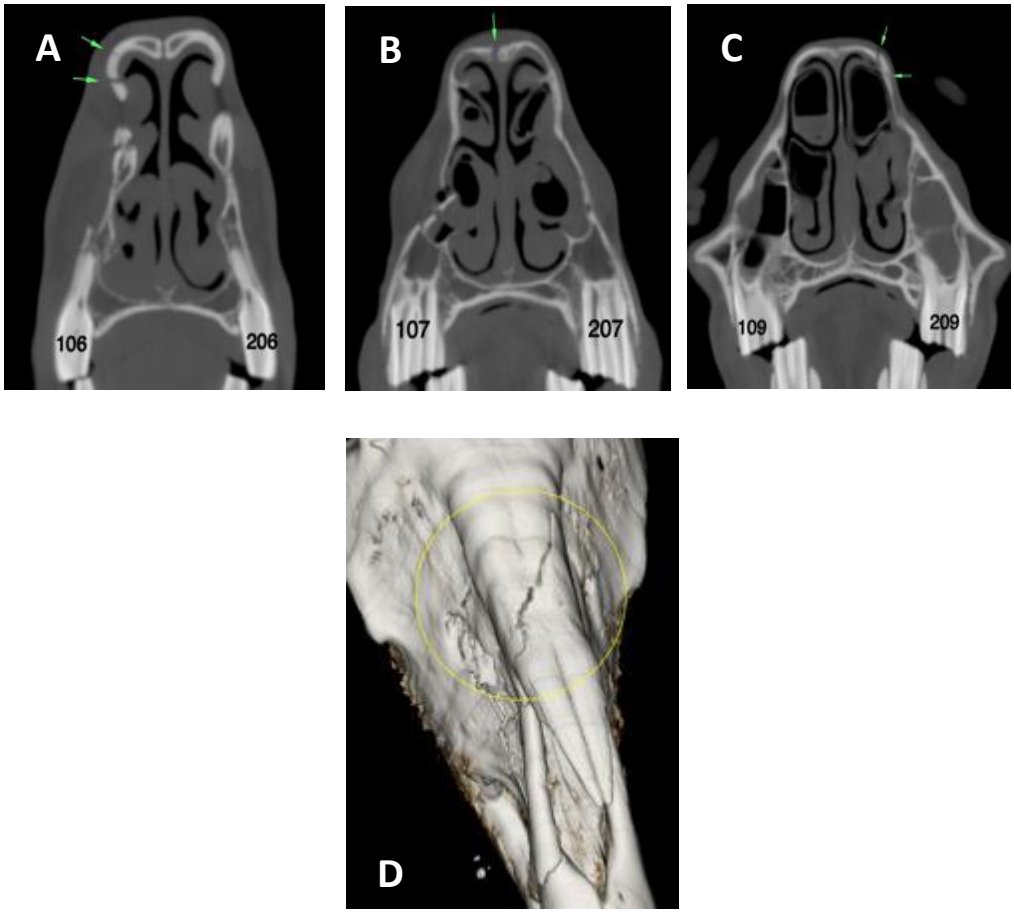

Figure 4. Transverse CT images (A., B. and C.) and three-dimensional reconstruction (D.) of the head. At the level of the right nasal bone there are two parallel fracture lines that originate at the ventrolateral border of the bone, dorsally to the nasoincisive notch (A.), and continue caudally (D.). The dorsal line is thinner and converge with the ventral line approximately at the level of 107 (B). From this point the fracture continues further caudomedially with a curve path (D.). At midline it crosses to the left nasal bone (C. and D.), where it continues caudolaterally until the level of 208, where it turns ventrally, and finishes at the level of the nasomaxillary suture. Right is to the left.

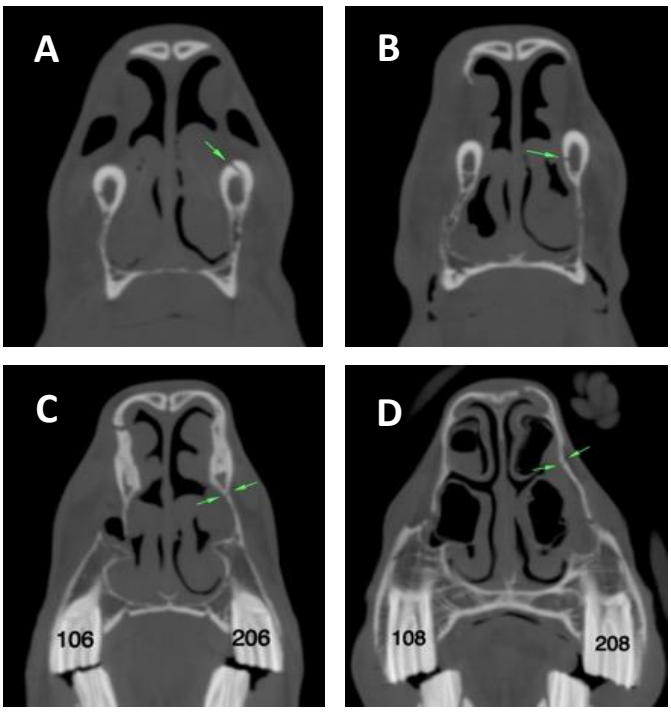

Figure 5. Transverse section CT images of the head. There is a thin fissure line that originates at the lateral cortex of the dorsal border of the nasal process of the left incisive bone at the level of the 204-206 interdental space (A). This line continues caudally turning towards the medial cortex (B). At the level of 206 joins the nasomaxillary suture (C) and continues caudally along the nasomaxillary suture (D.) until the level of 209, where it finishes. Right is to the left.

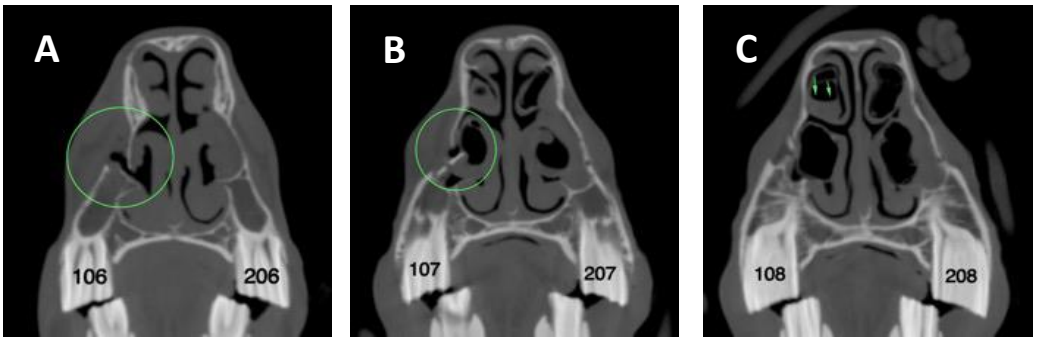

Figure 6. Transverse CT images (A., B. and C.) of the head. The right nasal passage is narrowed due to the displacement of the previously described fractures (green circles in A. and B.). There is moderate amount of soft tissue attenuating material (40 HU) within the dorsal and ventral nasal conchal bullae, this is more pronounced in the ventral one, where the dorsal border of the material is flat (fluid line). The ventral nasal conchal bulla contains several bone fragments from the maxillary bone fracture and there are areas of gas attenuation within the surrounding subcutaneous soft tissue, that are mildly swollen. Right is to the left of the images.

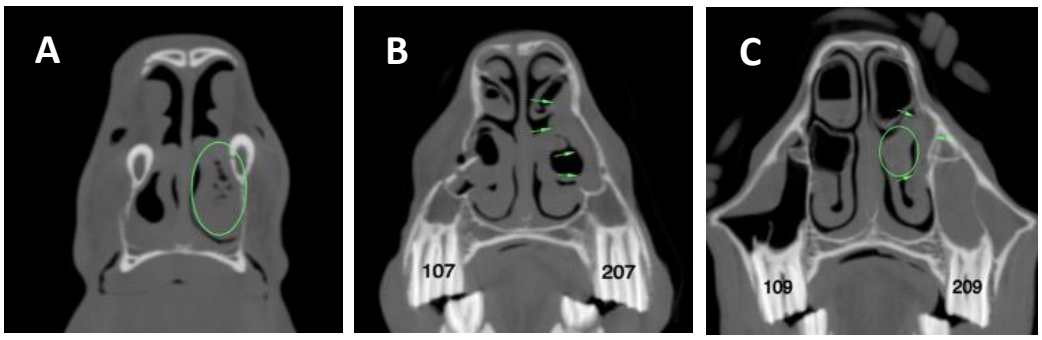

Figure 7. Transverse CT images (A., B. and C.) of the head. At the level of rostral aspect of the left ventral nasal concha there is moderate accumulation of heterogeneous soft tissue attenuating material with multiple interspersed gas bubbles (A.). From the level of 206 until the level of 210 there is a broad band (1-2 cm) of soft tissue attenuation (70 HU) at the medial aspect of the lateral wall of the nasal passage (left incisive, nasal and maxillary bones) (B.). There is also a small amount of material within the caudal aspect of the left ventral nasal conchal bulla (C.). Right is to the left of the images.

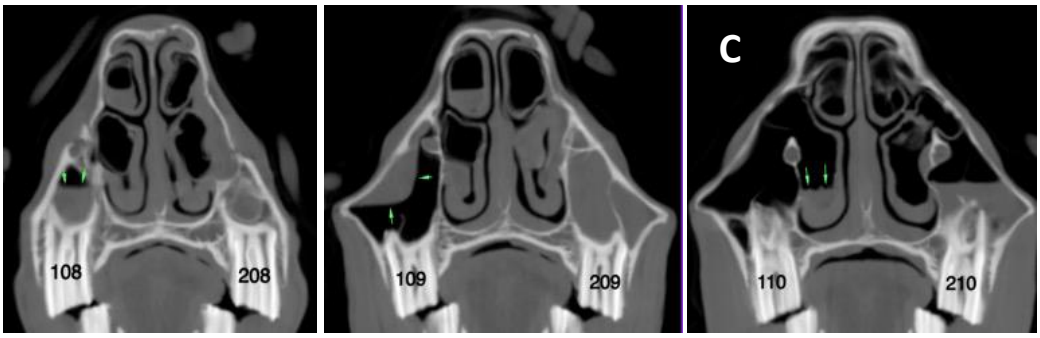

Figure 8. Transverse CT images (A., B. and C.) of the head. Within the right rostral sinus system (rostral maxillary and ventral conchal sinuses) there is soft tissue attenuating material (40 HU) accumulation in multiple locations: at the dependent aspect of the rostral maxillary sinus (A) and ventral conchal sinus (C), with a flat dorsal border (fluid line), and adhered to the medial aspect of the lateral wall (maxillary bone) of the rostral maxillary sinus (B.).
In the left rostral sinus system, there is abundant soft tissue attenuating material (30 HU) with a flat dorsal border that is filling the ventral half of the sinuses. In addition, in the area of the maxillary septal bulla there is moderate amount of heterogeneous soft tissue material with gas. There is gas within the infundibulum of 106, 109, 206, 209 and 210.